International Journal of Engineering and Geosciences
https://dergipark.org.tr/en/pub/ijeg
e-ISSN 2548-0960

Optimizing Land Image Classification: A Deep Learning Approach with ResNet-101 on the EuroSAT Dataset

Fatih Celik [*1], **Kemal Celik** [2]

[1] *Yildiz Technical University, Department of Geomatic Engineering, Istanbul 34210, Turkey, fatih.celik1@std.yildiz.edu.tr*
[2] *Department of Geomatics Engineering, Gumushane University, Gumushane, Turkey, gumuscelik@hotmail.com*

Cite this study: Çelik, F., Çelik, K., & Surname, N. (2025). Optimizing Land Image Classification: A Deep Learning Approach with ResNet-101 on the EuroSAT Dataset. International Journal of Engineering and Geosciences, 10 (2), 197-206.

https://doi.org/10.26833/ijeg.1538708

Keywords

Land Use
Land Cover
Eurosat Data
ResNet101
Squeeze synchronization
Data augmentation

Research Article

Received:26.08.2024
1.Revised: 05.12.2024
2.Revised: 25.12.2024
Accepted:25.01.2025
Published:01.07.2025

Abstract

The classification of image is essential to make LULC (Land Use Land Cover) maps. However, the classification of land cover plays a vital role for studying and modernizing the land areas. Recently, deep learning (DL) techniques have achieved outstanding performance in the classification of high-resolution images. Different techniques have been employed in traditional methods to identify LULC due to its complex and ever-changing nature. However, these studies have shown improved outcomes despite some restrictions such as inaccuracies and reduced performance. To address these problems, the proposed study introduces a Squeeze Synchronization Layer (SSL) and a Convolve Craft Focus Module (CCFM) where, SSL reduces input data complexity by removing noise and irrelevant information from images using pooling and convolutional operations also, CCFM enhances feature extraction to improve land classification accuracy. The EUROSAT land image dataset is utilized for the evaluation of the introduced model. Whereas, the dataset comprises of 64x64 images, which are captured by satellite Sentinel-2A in ResNet 101 input layer. Although, a SSL is suggested, and a CCFM is implemented in the convolutional layer for classifying land images. However, the efficiency of the system is evaluated by measuring performance metrics such as recall, F1-score, precision, and accuracy values of the proposed system. The accuracy value of the proposed system is 96% of accuracy, 100% of precision, 100% of recall, and 100% of F1-score, signifies the superior efficiency of the proposed model.

1. Introduction

Land Use and Land Cover (LULC) classification is essential for effective environmental management, urban planning, and resource allocation. It provides critical data for understanding land dynamics, assessing ecological changes, and implementing sustainable development practices [1]. LULC classification allows researchers and policymakers to monitor land transformation, which is crucial for addressing issues such as urban sprawl, deforestation, and climate change impacts [2]. Recent advancements in remote sensing and machine learning have significantly enhanced the accuracy of LULC classification [3, 4].

The Relation-Enhanced Multi scale Convolutional Network (REMSNet) incorporates parallel multi-kernel convolution and de-convolution modules in both encoding and decoding stages to capture features effectively [5, 6]. The integration of deep learning techniques in LULC classification highlights convolutional neural networks (CNNs), recurrent neural networks (RNNs), and hybrid models that combine traditional image processing with remote sensing and Geographic Information System (GIS) techniques for change detection and future predictions in urban areas [7, 8]. A three-layer classification scheme is employed for detailed urban land use and land cover classification at the metropolitan scale [9, 10]. Additionally, a Human Group-Based Particle Swarm Optimization (HG-PSO) algorithm with a Long Short-Term Memory (LSTM) classifier is utilized to classify land use and land cover [11, 12]. Quantitative analysis techniques evaluate the effectiveness of different distribution methods in urban planning [13, 14].

Moreover, (CNN) integrates (GIS) data for urban land-use classification [10, 15]. Effective incorporation of

remote sensing image categorization aids in the removal of spatiotemporal information for LULC classification [16, 17]. The methodology involves preprocessing satellite imagery followed by the application of algorithms such as Random Forest, Support Vector Machine, and Neural Networks. Deep learning techniques are applied for LULC classification using hyper spectral and multispectral earth observation data, assessing the performance of these methods for land cover classification and object detection on high-resolution remote sensing imagery [18, 19].

A comprehensive analysis of deep learning techniques, particularly CNNs, demonstrates their effectiveness in segmenting urban features from satellite imagery [20]. Deep learning semantic segmentation using Landsat 8 imagery employs CNN architecture to identify and classify different land cover types [21, 22]. However, an interpretable deep learning framework for LULC classification in remote sensing utilizes SHAP (Shapley Additive Explanations) with a compact CNN model to categorize satellite images, subsequently inputting outcomes to a SHAP deep explainer to reinforce image division results [23, 24]. Labelled samples are essential for achieving Land Cover Change Detection (LCCD) tasks through deep learning approaches with remote sensing images; however, labelling samples for change identification with bi-temporal remote sensing images is time-consuming and labor-intensive [25, 26]. Research on future LULC detection has been conducted across Mumbai and its surrounding areas in India to support urban development [27]. To achieve insights into LULC's historical dynamics, a supervised classification algorithm is implemented on Landsat images from 1992, 2002, and 2018 [28, 29]. Further the study SFN (Street-Frontage-Net), CNN been developed in order to assess the quality of street frontage as either being blank frontage containing fences, garages and walls or active frontage comprising doors as well as windows [30].

Furthermore, thirty-nine Deep Transfer Learning models are systematically assessed under consistent conditions for LULC classification [31]. Remote sensing data combined with a Cellular Automata Markov (CA-Markov) model is utilized to assess land use and land cover change detection and prediction in the northern coastal districts of Tamil Nadu, India [32]. A Cellular Automata-Artificial Neural Network (CA-ANN) simulation assesses LULC changes using the CA model to simulate spatial changes while integrating ANN to predict future land use scenarios [33]. Satellite images from 1991 to 2021 are analyzed to produce LULC maps using SVM classification in ArcGIS across six categories: developed, barren, forest, wetlands, and water [34]. Also, the study aimed to evaluate and detect the urban development of the Peshawar region and LULC with a CA (Cellular Automata- Markov-Chain) [35, 36].

Also an approach utilized Landsat imagery to assess and predict land use/land cover changes, land surface temperature and the urban thermal field variance index for the Dhaka Metropolitan area. CA model combined with the Patch-Generating Land Use Simulation model to forecast urban land use change [23, 34].The study of modern multi-OCNN (Multi-scale OCNN) framework for big-scale land cover classification [37, 38]. Also, the study aimed at detecting LST (Land-Surface-Temperature) and LULC with a CA-Markov-Chain [36]. Furthermore, the study has been investigated the application of DSVM (Deep Support Vector Machine) for classification of hyper-spectral image [39]. Also the former method of the study includes pixel based classification with CNN by using the Flickr API and pre-trained ResNet18 employed to recognize land use classes [40, 41]. Furthermore, CNN-DL neural networks have been utilized for classification of land use in satellite enhanced with better differentiation [42]. Similarly, unsupervised learning algorithms to cluster hybrid polarimetric and dual-polarized SAR images by extraction of layers from the VGG-16 indicates effective classification performance in land images [43].

As a result, the existing studies conducted on the Prediction of Land Image Classification have shown different methods for LULC. Nonetheless, these traditional studies encounter significant limitations in complex applications, primarily due to their inability to manage high dimensionality, which can cause overfitting and hinder predictive capabilities. These models struggle to integrate spatial and non-spatial factors, failing to capture intricate data relationships, diminishing performance. Additionally, the lack of labeled data presents challenges, as traditional methods depend heavily on extensive labeled datasets. Proposed model aimed to overcome these limitations via advanced techniques like data augmentation and robust feature extraction, enhancing generalization and classification accuracy in remote sensing. So in order to address these issues, the proposed model utilizes processes pre-processed images from the EuroSAT dataset through the ResNet 101 architecture, known for its deep feature learning. A layer SSL compresses the data, filtering out noise to enhance quality. The CCFM improves feature extraction via adaptive convolutions and capturing intricate patterns of land cover types. Also, Non-linear activation functions support learning of complex relationships. The output layer produces classification probabilities for ten land cover classes. Where the training phase optimizes the model using cross-entropy loss and Adam optimizer. Finally, the prediction phase evaluates performance metrics like accuracy and F1-score. In summary, the improvements in these methods have overcome these limitations and set a benchmark for land cover classification tasks over other traditional methods.

2. Proposed Methodology

The proposed method uses the land cover image dataset for determining the categorization of land images. Although, Conventional machine learning models often face difficulties when handling high-dimensional data, leading to problems like over fitting or poor performance. Numerous earlier models have had difficulty effectively incorporating both spatial and non-spatial elements, hindering their capacity to grasp the

complete complexity of the data. The original ResNet-101 drawback of this model is its computational complexity and the high demand for resources. The intricate architecture of the ResNet-101 model makes it more challenging to train from scratch, requiring a substantial amount of data and extended training time to reach optimal performance levels. This complexity can hinder its deployment in resource-constrained environments, where efficiency and speed are critical. Consequently, addressing these issues will be essential for improving the model's accessibility and usability in practical applications. By concerning this challenges the proposed model is primarily evaluated on the EUROSAT dataset for pre-processing, training and testing phases. Where the classification is done by the SSL and CCFM in ResNet input layer and convolution layer, respectively. The main goal of the SSL is to streamline input information by eliminating unnecessary noise and irrelevant data using pooling and convolutional techniques. This assists models in concentrating on essential features to enhance accuracy and minimize computational workload. The CCFM improves feature extraction in image data for more precise classification of land cover types.

The model architecture begins with an input layer that accepts the pre-processed images into the ResNet 101 framework. A SSL follows, which compresses the input data to filter out noise and irrelevant details. This is succeeded by the CCFM, enhancing feature extraction through adaptive convolutional operations that allow for the capture of intricate patterns associated with various land cover types. Non-linear activation functions are utilized to enable the model to learn complex relationships within the data, culminating in an output layer that produces classification probabilities for ten distinct land cover classes. During the training phase, the model is optimized using a combination of cross-entropy loss and algorithms like Adam to minimize classification errors. This progress enables a deeper comprehension of the data, resulting in enhanced performance and dependability across multiple applications. Finally, in the prediction phase, the model's effectiveness is assessed on the test dataset through performance metrics such as accuracy, F1-score, precision, and recall.

Figure 1 the flowchart diagram outlines a comprehensive machine learning or deep learning workflow specifically designed for processing and classifying land cover images, organized into several sequential steps. It begins with the Loading the EuroSAT dataset phase, where a collection of images representing various land cover types is introduced forming the basis for subsequent training and testing. The workflow then progresses to the Pre-processing stage, which is divided into three essential sub-steps: Image Resizing, ensuring uniform dimensions across all images; Normalization, which adjusts pixel values to a standard scale (typically between 0 and 1) and data augmentation where additional variations of the dataset are created through techniques like rotation and flipping to enhance model robustness and mitigate over fitting.

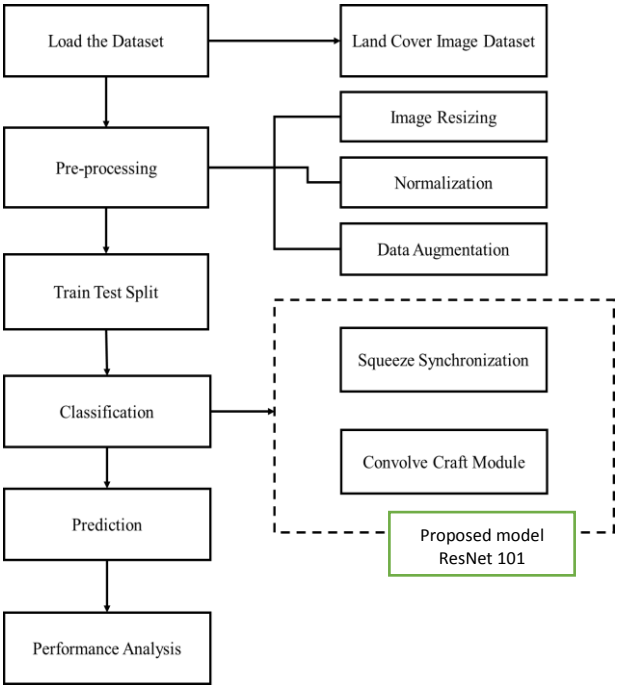

Figure 1. Overall Flow of the Proposed Model

Following preprocessing, the train-test split step divides the dataset into training and testing subsets, allowing for effective model evaluation. For the training and testing phases, the data has been collected from the EuroSAT dataset. However, the model is trained using a combination of cross-entropy loss and optimization algorithms Adam optimizer to minimize classification errors. The Classification phase applies a machine learning or deep learning model to categorize the land cover images, incorporating components such as Squeeze Synchronization to reduce dimensionality and the Convolve Craft Module for feature extraction. Next, the Prediction step translates the model's outputs into interpretable results regarding land cover types. Finally, the workflow culminates in Performance Analysis, where various metrics—such as accuracy, precision, and recall—are employed to assess the model's reliability and effectiveness. Overall, this structured approach is particularly relevant for applications in remote sensing, environmental monitoring, and geospatial analysis, highlighting its significance in land cover classification tasks.

2.1. Dataset Description

LULC classification is used to find the class of remote sensing image regarding some well-defined target class labels. For training the suggested model, EuroSAT dataset is used, which is now a typical benchmark for land-cover categorization tasks. This dataset, sourced from Kaggle, comprises approximately 27,000 labeled images categorized into ten distinct classes. Each image has dimensions of 64x64 pixels and was captured with Sentinel-2A satellite 4 years ago, the data in EuroSAT consists of multi-spectral images with 13 spectral bands.

In the training phase, the model employs a combination of cross-entropy loss and optimization algorithms like the Adam optimizer to minimize classification errors effectively. Following this, in the prediction phase, the model is evaluated against a test

dataset, with performance metrics such as accuracy, F1-score, precision, and recall calculated to assess its effectiveness. The corresponding section deals with the data used in the corresponding study with their appropriate data link for further reference.

https://www.kaggle.com/code/rajaraman6195/land-cover-classification

2.2. Image Pre-Processing

Typically, the model becomes increasingly complex when processing all the data attributes extracted from the raw input data for each dataset. The dataset of images is employed in this proposed study. The image pre-processing phase plays a crucial role in the proposed model to enhance the training of input data to produce optimal solutions and performance. The pre-processing phase in this study encompasses three key steps including image resizing, normalization, and data augmentation.

Changing an image's dimensions while preserving its aspect ratio is the essence of image resizing. This process can involve either increasing the image's size by scaling up its pixel dimensions or decreasing its size by scaling down its pixel dimensions. The proposed model utilizes the open-source library CV2 for image resizing operations. Due to its ability to resize and maintain aspect ratio, it is also employed for improved visibility in presentations and computer vision applications.

The technique of normalization is used in image processing to control the pixel value of an image. To guarantee the effectiveness of image analysis algorithms, pixel values need to be normalised to a standardised range, typically between 0 and 1. Normalizing pixel values minimizes the impact of variations in lighting conditions, contrast, and color. This technique enhances the image data, making it more compatible for machine learning applications such as object detection or image classification.

The proposed model utilizes the Image Data Generator to enhance image classification models through Data Augmentation, as implemented in Keras to augment the training dataset. Techniques such as rotation, width and height shifts, zooming, sharing, and flipping are included to prevent overfitting and enhance generalisation. These methods result in more robust models, which improve precision and resilience across a wide range of conditions and datasets, ultimately increasing model effectiveness.

3. Data Splitting

It is the procedure, which refers to the method of partitioning a dataset into individual subsets for validation, testing and training procedures in ML. whereas, it is a critical process in ML, involving dividing the dataset into various subsets. It is essential for training models, tuning parameters, and ultimately evaluating its performance. In the proposed study, the pre-processed data is split into two sets, one is train split (80%) and the other is test split (20%). Hence, data splitting is essential to eliminate any bias in the subsets.

3.1. Proposed ResNet 101 Architecture

ResNet101 is a deep CNN architecture, which belongs to the ResNet (Residual Network) family. It specifically refers to a ResNet model with 101 layers, which includes a series of convolutional, pooling, and completely connected layers. It is known for their deep structure and the utilization of residual connections. ResNet-101 has been widely utilized for different computer vision operations, like image classification and segmentation as well as object detection, due to its robust performance and ability to learn complex features from visual data. Though ResNet-101 model has advantages, it also possesses some limitations. The one of the major limitations of this model is its computational complexity and the requirement of resources. Also, ResNet-101 model makes it more challenging to train from scratch, requiring more data and longer training time to attain optimal performance. Hence, the model has been proposed with the SSL and CCFM model to enhance the efficiency of land image classification. Figure 2 demonstrates the unveiling SSL and CCFM in ResNet 101 model.

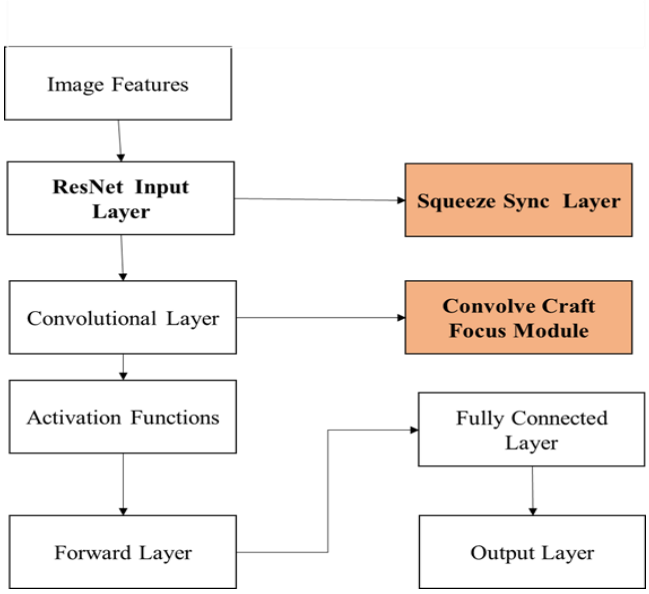

Figure 2. Unveiling SSL and CCFM – ResNet 101 Model

The featured images have been entered into the ResNet input layer, where the classification occurred. In the ResNet layer, the SSL is proposed. Squeeze synchronization is a component used in DL models, particularly in the context of neural networks. Its operation is to compress the input data by eliminating its dimensionality, typically through techniques like pooling or convolution. Simply, SSL acts as a critical part in improving the accuracy and efficiency of neural networks by streamlining the information flow and reducing the overall computational load. In the introduced model, SSL is proposed to avoid the noisy and blurry features from the images in the dataset. After that, the features enter the convolutional layer, where the meaningful features are mined from input images and are essential for the success of CNNs in different computer vision applications. In the convolutional layer, the CCFM is introduced. CCFM is suggested in the proposed system to

enhance the feature extraction. The extracted features are then entered into the activation functions layer, which play an important role in the DL model by allowing them to learn complex patterns and associations in the image and finally enter the output layer.

In the proposed system, the conventional ResNet 101 model is improved by introducing the novel CCFM for the better prediction of land image classification. CCFM is a craft focus module, which is embedded in the convolutional layer of the proposed ResNet 101 model.

$$y = \text{softmax}\,(em^K + en^K)v \quad (1)$$

Where is the output of the CCFM block, and $em^K + en^K$ are the craft focus modules.

Figure 3 reveals the structural comparison of the traditional ResNet 101 structure model to the proposed ResNet 101 model structure.

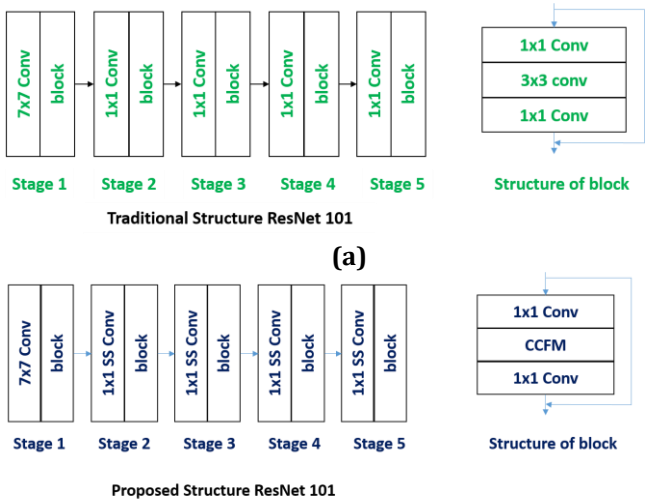

Figure 3. (a) Traditional ResNet 101 Architecture (b) Proposed Model ResNet 101 Architecture

Traditional ResNet 101 and the proposed ResNet 101 models vary in the last bottleneck only. Figure 3 shows the structural comparison of the two bottlenecks. Figure 3 (a) reveals the last bottleneck structure of the original ResNet 101 model, whereas Figure 3(b) shows the improvement in the bottleneck by incorporating CCFM. Generally, conventional ResNet 101 contains five stages, which are altered in proposed ResNet 101 model. The proposed ResNet 101 model replaces 3 × 3 convolution in the last bottleneck block of the proposed ResNet 101 model with CCFM blocks. Similarly, stage 2, 3 and 4 consist of 3, 4, 6 and 3 residual blocks, respectively. The proposed structure seeks to enhance or modify this traditional design by substituting one critical layer, the 3x3 convolution, with a potentially more efficient and powerful module known as CCFM.

This approach underscores a prevalent strategy in deep learning research: building upon successful architectures like ResNet while implementing targeted modifications aimed at improving performance. By integrating CCFM, architecture aspires to refine feature representation and overall model efficacy, reflecting the ongoing trend of advancing deep learning technologies through strategic enhancements to established frameworks. Which could indicate a reduction in parameters, focus on different types of feature processing and potentially improved generalization for faster inference. The overall proposed model is shown in figure 4.

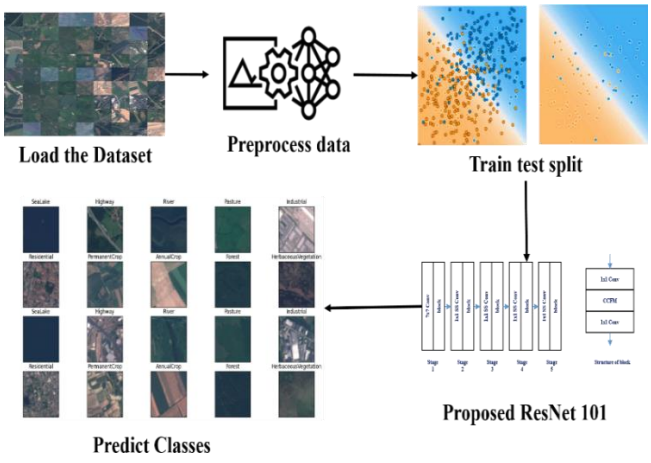

Figure 4. Overall Proposed System

The complete proposed system is revealed in figure 4. In the proposed model, the EuroSAT image dataset is loaded into the system and loaded dataset is entered into the model testing and training phase. In this phase, the dataset is divided into two parts, one is for testing and the other is for training. After this phase, the image dataset is processed, and the classification of image dataset is determined.

4. Results and Discussion

The outcomes generated by execution of introduced SSL and CCFM which are deliberated in this section. Besides performance metrics, performance analysis and EDA are also discussed. In addition, the comparison of conventional techniques with the proposed system is also described to reveal the efficiency of the introduced model.

4.1. Performance Metrics

The efficiency of the proposed model is assessed by the performance metrics namely F1 (F1 score), R (recall), A (accuracy) and P (precision) values. The performance metrics can be described in the corresponding equation.

F1-Score: It is derived by the mean assessment of the values of precision and recall values. The classifier quality is also enhanced, if F1 score is greater, which is given by the equation (2)

$$F1 = 2 * \frac{\text{Recall} * \text{Precision}}{\text{Recall} + \text{Precision}} \quad (2)$$

Recall: It is defined as the ratio of the precisely identified results to overall findings, which is given by equation (3),

$$R = \frac{True_{positive}}{False_{negative} + True_{positive}} \quad (3)$$

Accuracy: The ratio of the precise detection of samples to the overall identification of the classifier. The formula for accuracy is described in the formula (4),

$$A = \frac{True_{positive} + True_{negative}}{True_{positive} + False_{positive} + True_{negative} + False_{negative}} \quad (4)$$

Precision: It is the ratio of the values of true positive to the combination of false positives and true positives, which is given by equation (5),

$$P = \frac{True_{positive}}{True_{positive} + False_{positive}} \quad (5)$$

Where, TN($True_{negative}$) denotes the number of negative samples, which are found precisely. TP ($True_{positive}$) represent the total amount of precisely found samples, FP ($False_{positive}$) denotes the total amount of positive samples, which are imprecisely found and the FN($False_{negative}$) determines the quantity of negative samples, which are imprecisely found.

4.2. EDA (Exploratory Data Analysis)

It is a process of using descriptive statistics and graphical tools that help in understanding the data in a better way. Since, it is used to maximize the insights of dataset and find the anomalies, outliers and then assess the underlying assumptions. EDA of the proposed system maximizes the insights of the image datasets and detects the anomalies and characteristics of the image dataset. Figure 5. Depicts the EDA for EuroSAT class distribution.

The proposed study uses ten different land images of different sizes, which are shown in figure 5. The x-axis of the graph denotes the class labels, whereas the y-axis of the graph represents the size of the classes.

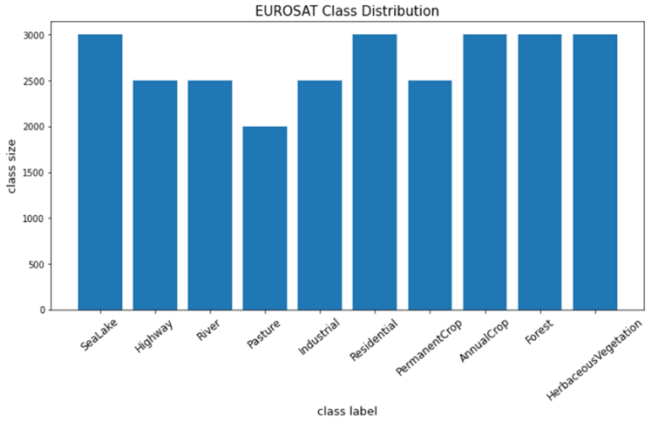

Figure 5. EDA for EUROSAT Class Distribution

The majority of the class labels are typically larger in size, originating from the dataset. Analysis of the EUROSAT data distribution is conducted using EDA.

4.3. Performance Analysis

It refers to the method of assessing and examining the performance of the suggested model. However, the performance analysis is assessed using confusion matrix of the proposed system. In addition, the graphs for model accuracy and loss are also deliberated. Confusion matrix explains the execution of the algorithm of classification. Generally, a confusion matrix summarizes and visualizes the execution of a classification algorithm. Performance analysis of the introduced work is depicted in subsequent section. Figure 6 reveals the confusion matrix of the suggested model.

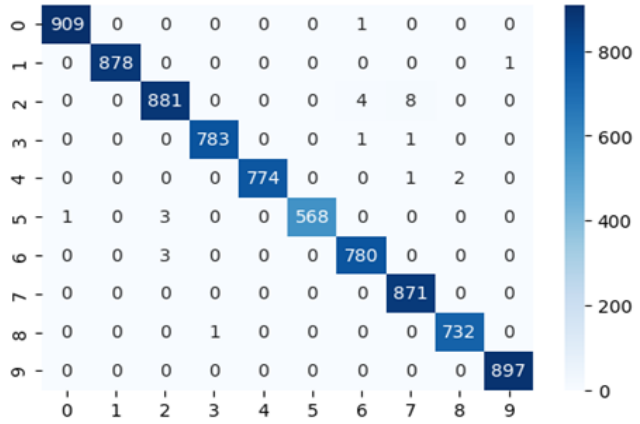

Figure 6. Confusion Matrix of the Proposed Model

The performance of the classification model can be summarized using a confusion matrix, which compares predicted labels with actual labels in figure 6. In the land image classification scenario, predicted labels are referred to the classification of land images, whereas the actual labels denote the ground truth. In multi-class confusion matrix, the rows denote the actual labels, and the columns denote predicted labels. In confusion matrix, each cell represents the number of instances falling into a specific predicted-actual label combination. Also, while performing in multiple classes the results gave high accuracy, precision, Recall, F1 rates with 0.99 and 1 respectively. Hence, the multi-class confusion matrix enables a detailed assessment of the performance of land image classification, conferring an accuracy metric as well as predicting accurate land image classification. By examining the confusion matrix, developers can find patterns and trends in misclassified data, helping to improve image classification. In addition, multi-class classification can be used to assess other performance metrics. Figure 7. Reveals the graphical representation of loss and accuracy for the proposed model.

Figure 7 depicts the accuracy values of the proposed research model, which can be classified into two categories: validation accuracy and training accuracy. The training loss of the model is denoted by a blue graph, whereas its validation accuracy is denoted by an orange graph (a). Whereas the validation and training loss of the model is represented in (b). Its training accuracy is depicted by a blue graph, and its validation accuracy is depicted in orange.

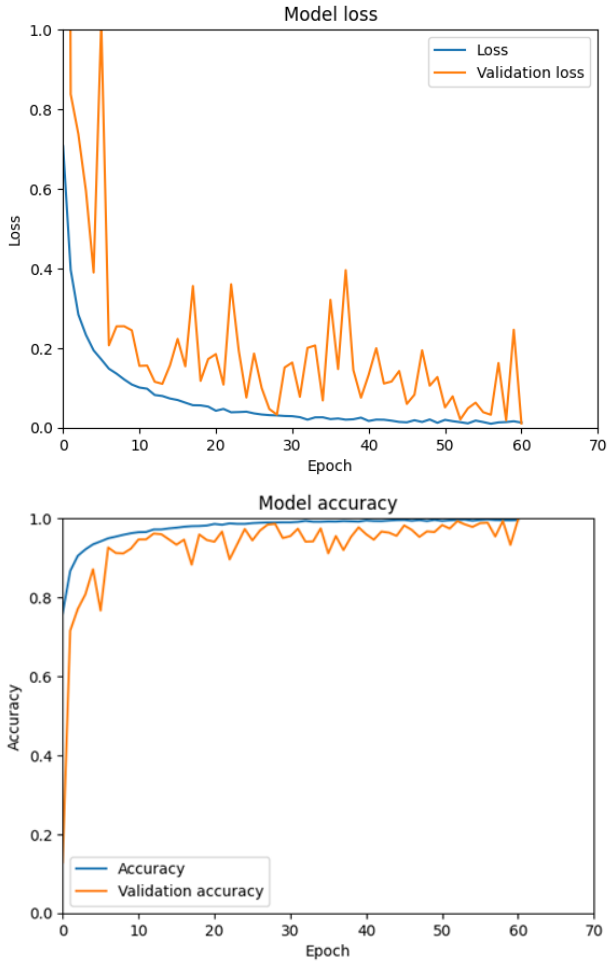

Figure 7. (a) Model Loss (b) Model Accuracy

In general, it is a process of parallel comparison that methodically compares multiple things to highlight its resemblances and variances. Also, it is the method of comparing the introduced model with the existing algorithms to assess the complete execution of the introduced model.

In internal results, the values of each performance metric for each class are calculated. Table 1 depicts the internal outcomes of the suggested model. The classification report of the different classes is described in table 1 and figure 8. In table 1, precision (P), recall (R), F1-score (F1) and accuracy (A) are calculated.

Table 1. Outcome of Different Classes

Classes	Precision	Recall	F1-Score
0	1	1	1
1	1	1	1
2	0.99	0.99	0.99
3	1	1	1
4	1	1	1
5	1	0.99	1
6	0.99	1	0.99
7	0.99	1	0.99
8	1	1	1
9	1	1	1

Table 1 indicates the internal outcomes of the proposed system from various classes from 0 to 9, which are different types of land images. Classes 0, 1, 2, 3, 4, 5, 6, 7, 8 and 9 are annual crop, forest, herbaceous vegetation, highway, industrial, pasture, permanent crop, residential, river and sea lake land images, respectively. Precision, recall and F1-score are the performance metrics that are taken for different land images. The graphical representation of the classification report of various classes is revealed in Figure 8.

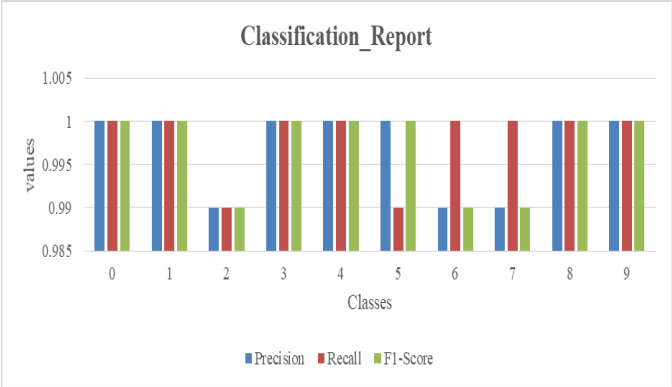

Figure 8. Classification Report on the Different Classes

The comparison of the outcomes of existing methods with the proposed method is tabulated in table 2. The comparison of the performance metric of the existing methods with the proposed method are deliberated below.

Table 2. Comparison of Existing Models with the Proposed Model

Model	Accuracy
VGG16(Without augmentation	0.9814
VGG16(With augmentation)	0.9855
WideResNet-50(Without augmentation)	0.9904
WideResNet-50(With augmentation)	0.9917
Proposed Model	0.9966

The value of the accuracy of the existing models are compared with the accuracy value of the projected system, which are revealed in table 2. The maximum accurate value of the existing system is 0.9917, whereas the proposed system achieves the accuracy of 0.996. It indicates that the suggested model is more accurate than the other traditional methods.

Table 3. Comparison of Existing Models with the Proposed Model

Model	Accuracy
Google Net	0.9669
Hybrid Feature Optimization Algorithm with DL Classifier	0.9740
Proposed Model	**0.9966**

In table 3, the accuracy values of the conventional methods with the accuracy values of the introduced model. The maximum accuracy value of the conventional model is 0.97, while the introduced model attains the accuracy of 0.996. This reveals that the projected methods confer better performance than the conventional models.

Table 4. Performance analysis of proposed model over traditional model

Model	Accuracy	Precision	F1-score	Recall
Traditional	0.9700	0.9700	0.9700	0.9700
Proposed	0.9966	1.0000	1.0000	1.0000

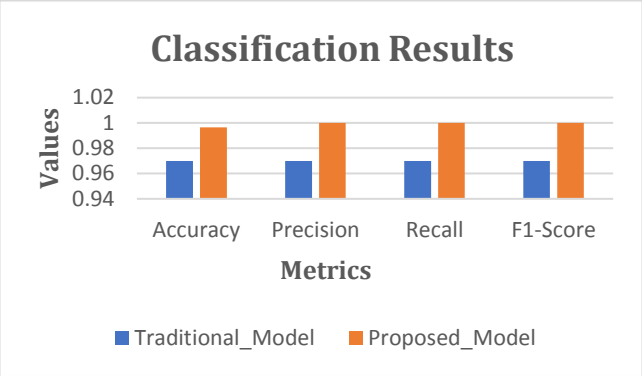

Figure 8. Graphical representation of Table 4

Table 4 and Figure 8 depicts the traditional ResNet 101 model accuracy, precision, recall and F1 score over proposed ResNet 101 with CCFM model. The proposed outcome has showed higher 0.9966 in terms of accuracy

5. Discussion

The suggested research highlights a notable progress in land image classification by incorporating novel methods into the ResNet 101 model. Although the initial ResNet-101 model presents numerous benefits, it also has significant drawbacks. A significant drawback is its computational complexity and resource demands, which may limit its use in practical situations. Moreover, training the ResNet-101 model from the ground up present's difficulties, since it requires significant amounts of data and prolonged training durations to reach peak performance. To tackle these challenges, the research presents improvements by integrating the SSL and the CCFM. The SSL optimizes input data by removing noise and irrelevant details through pooling and convolution operations, enabling the model to concentrate on vital features for enhanced accuracy while lessening computational demands. At the same time, the CCFM improves feature extraction abilities, allowing for more efficient distinction among land cover types, resulting in superior classification results. The model effectively addresses issues related to high-dimensional data, achieving a remarkable accuracy of 0.996, while the traditional ResNet achieves 0.97 accuracy rate. Highlighting its excellent performance in comparison to conventional techniques. This underscores its possibilities for multiple uses such as natural resource management, urban development, and environmental observation. Upcoming efforts will focus on simplifying the model to improve efficiency and robustness.

6. Conclusion

In conclusion, the proposed study demonstrates a significant advancement in land image classification through the integration of innovative techniques within the ResNet 101 model. By incorporating the SSL and CCFM. The SSL seeks to streamline input data by eliminating noise and unnecessary details via pooling and convolution operations. This aids models in concentrating on key traits for better accuracy and decreased computational load. The CCFM improves feature extraction in image data to more effectively differentiate land cover types for improved classification outcomes. The model effectively addresses challenges associated with high-dimensional data, enhancing accuracy and reducing computational load while minimizing over fitting. The achieved accuracy of 0.996 underscores the model's superior performance compared to traditional methods, highlighting its potential for various applications in natural resource management, urban planning, enhanced accuracy, increased robustness, computational efficiency, improved interpretability and environmental monitoring. Future work focus on model optimization and simplification to enhance the efficiency. This future work will focus on investigating lightweight architectures that employ knowledge distillation techniques to develop smaller and faster models capable of maintaining performance while being suitable for deployment on edge devices. Additionally, the research will explore the model's effectiveness using various datasets to enhance its robustness and adaptability. This ongoing commitment to refinement is expected to produce even more reliable and efficient tools for land use and land cover mapping, ultimately contributing to improved decision-making in resource management and environmental stewardship.

Author contributions

Fatih Celik: Conceptualization, Methodology, Software, Field study, Data curation, Writing-Original draft preparation, Software, Validation., Field study **Kemal Celik:** Visualization, Investigation, Writing-Reviewing and Editing.

Conflicts of interest

The authors declare no conflicts of interest.

References

1. Ayalke, Z., & Şişman, A. (2024). Google Earth Engine kullanılarak makine öğrenmesi tabanlı iyileştirilmiş arazi örtüsü sınıflandırması: Atakum, Samsun örneği. Geomatik. https://doi.org/10.29128/geomatik.1472160
2. Esen, Ö., Çay, T., & Toklu, N. (2017). Evaluation Of Land Reform Policies In Turkey. International Journal Of Engineering And Geosciences, 2(2), 61–67. https://doi.org/10.26833/ijeg.297223
3. Noi Phan, T., Kuch, V., & Lehnert, L. W. (2020). Land cover classification using google earth engine and random forest classifier-the role of image

composition. Remote Sensing, 12(15). https://doi.org/10.3390/RS12152411
4. Serwa, A. (2020). Studying the Potentiality of Using Digital Gaussian Pyramids in Multi-spectral Satellites Images Classification. Journal of the Indian Society of Remote Sensing, 48(12), 1651–1660. https://doi.org/10.1007/s12524-020-01173-w
5. Liu, C., Zeng, D., Wu, H., Wang, Y., Jia, S., & Xin, L. (2020). Urban land cover classification of high-resolution aerial imagery using a relation-enhanced multiscale convolutional network. Remote Sensing, 12(2). https://doi.org/10.3390/rs12020311
6. Isazade, V., Isazade, E., Qasimi, A. B., & Serwa, A. (2023). Integrating Passive and Active Remote Sensing Data with Spatial Filters for Urban Growth Analysis in Urmia, Iran. Russian Journal of Earth Sciences, 23(5). https://doi.org/10.2205/2023ES000861
7. Zhao, S., Tu, K., Ye, S., Tang, H., Hu, Y., & Xie, C. (2023, November 3). Land Use and Land Cover Classification Meets Deep Learning: A Review. Sensors (Basel, Switzerland). https://doi.org/10.3390/s23218966
8. Paul, S. (2022). Change detection and future change prediction in Habra I and II block using remote sensing and GIS – A case study. International Journal of Engineering and Geosciences, 7(2), 191–207. https://doi.org/10.26833/ijeg.975222
9. Unel, F. B., Kusak, L., & Yakar, M. (2023). GeoValueIndex map of public property assets generating via Analytic Hierarchy Process and Geographic Information System for Mass Appraisal: GeoValueIndex. Aestimum, 82, 51-69
10. Çay, T., & Satılmış, R. Y. (2024). Economic Analysis of Land Consolidation Project: Kızılcabölük Neighborhood, Tavas- Denizli- Turkey Province. International Journal of Engineering and Geosciences. https://doi.org/10.26833/ijeg.1429522
11. Babu, R. G., Maheswari, K. U., Zarro, C., Parameshachari, B. D., & Ullo, S. L. (2020). Land-Use and Land-Cover Classification Using a Human Group-Based Particle Swarm Optimization Algorithm with an LSTM Classifier on Hybrid Pre-Processing Remote-Sensing Images. Remote Sensing, 12(24), 1–28. https://doi.org/10.3390/rs12244135
12. Hazer, A., Bozdağ, A., & Atasever, Ü. H. (2024). Hiper-Optimize Edilmiş Makine Öğrenim Teknikleri ile Taşınmaz Değerlemesi, Yozgat Kenti Örneği. Geomatik. https://doi.org/10.29128/geomatik.1454915
13. Eyi, G., & Buğdaycı, İ. (2024). Uzaktan Algılama Yöntemleri ile Yangın Şiddetinin Tespiti: Yunanistan Rodos Adası Orman Yangını Örneği. Geomatik. https://doi.org/10.29128/geomatik.1481708
14. Güngör, R., & İnam, Ş. (2019). İmar Uygulamalarında Farklı Dağıtım Metotlarının Karşılaştırılması. Geomatik, 4(3), 254–263. https://doi.org/10.29128/geomatik.548592
15. Yu, J., Zeng, P., Yu, Y., Yu, H., Huang, L., & Zhou, D. (2022). A Combined Convolutional Neural Network for Urban Land-Use Classification with GIS Data. Remote Sensing, 14(5). https://doi.org/10.3390/rs14051128
16. Amini, S., Saber, M., Rabiei-Dastjerdi, H., & Homayouni, S. (2022). Urban Land Use and Land Cover Change Analysis Using Random Forest Classification of Landsat Time Series. Remote Sensing, 14(11). https://doi.org/10.3390/rs14112654
17. Savanović, R., & Savanović, M. (2024). The need for renewal of the real estate cadastre on the territory of Vojvodina, Republic of Serbia. International Journal of Engineering and Geosciences. https://doi.org/10.26833/ijeg.1422964
18. Abdi, A. M. (2020). Land cover and land use classification performance of machine learning algorithms in a boreal landscape using Sentinel-2 data. GIScience and Remote Sensing, 57(1), 1–20. https://doi.org/10.1080/15481603.2019.1650447
19. Şenol, H. İ., Kaya, Y., Yiğit, A. Y., & Yakar, M. (2024). Extraction and geospatial analysis of the Hersek Lagoon shoreline with Sentinel-2 satellite data. *Survey Review*, *56*(397), 367-382.
20. Neupane, B., Horanont, T., & Aryal, J. (2021, February 2). Deep learning-based semantic segmentation of urban features in satellite images: A review and meta-analysis. Remote Sensing. MDPI AG. https://doi.org/10.3390/rs13040808
21. Boonpook, W., Tan, Y., Nardkulpat, A., Torsri, K., Torteeka, P., Kamsing, P., … Jainaen, M. (2023). Deep Learning Semantic Segmentation for Land Use and Land Cover Types Using Landsat 8 Imagery. ISPRS International Journal of Geo-Information, 12(1). https://doi.org/10.3390/ijgi12010014
22. Rajmohan, G., Chinnappan, C. V., John William, A. D., Chandrakrishan Balakrishnan, S., Anand Muthu, B., & Manogaran, G. (2021). Revamping land coverage analysis using aerial satellite image mapping. Transactions on Emerging Telecommunications Technologies, 32(7). https://doi.org/10.1002/ett.3927
23. Faisal, A. Al, Kafy, A. A., Al Rakib, A., Akter, K. S., Jahir, D. M. A., Sikdar, M. S., … Rahman, M. M. (2021). Assessing and predicting land use/land cover, land surface temperature and urban thermal field variance index using Landsat imagery for Dhaka Metropolitan area. Environmental Challenges, 4. https://doi.org/10.1016/j.envc.2021.100192
24. Tariq, A., & Shu, H. (2020). CA-Markov chain analysis of seasonal land surface temperature and land use landcover change using optical multi-temporal satellite data of Faisalabad, Pakistan. Remote Sensing, 12(20), 1–23. https://doi.org/10.3390/rs12203402
25. Lv, Z., Huang, H., Sun, W., Jia, M., Benediktsson, J. A., & Chen, F. (2023). Iterative Training Sample Augmentation for Enhancing Land Cover Change Detection Performance With Deep Learning Neural Network. IEEE Transactions on Neural Networks and Learning Systems. https://doi.org/10.1109/TNNLS.2023.3282935
26. Dinda, S., Das Chatterjee, N., & Ghosh, S. (2021). An integrated simulation approach to the assessment of urban growth pattern and loss in urban green space in Kolkata, India: A GIS-based analysis. Ecological

Indicators, 121. https://doi.org/10.1016/j.ecolind.2020.107178
27. Vinayak, B., Lee, H. S., & Gedem, S. (2021). Prediction of land use and land cover changes in Mumbai city, India, using remote sensing data and a multilayer perceptron neural network-based Markov Chain model. Sustainability (Switzerland), 13(2), 1–22. https://doi.org/10.3390/su13020471
28. Kadı, F., & Yılmaz, O. S. (2024). Determination of alternative forest road routes using produced landslide susceptibility maps: A case study of Tonya (Trabzon), Türkiye. International Journal of Engineering and Geosciences, 9(2), 147–164. https://doi.org/10.26833/ijeg.1355615
29. Yilmaz, O. S., Gülgen, F., Güngör, R., & Kadi, F. (2018). Coğrafi Bilgi Sistemleri ve Uzaktan Algılama Teknikleri İle Arazi Kullanım Değişiminin İncelenmesi, Köprübaşı İlçesi Örneği. Geomatik, 3(3), 233–241. https://doi.org/10.29128/geomatik.410987
30. Law, S., Seresinhe, C. I., Shen, Y., & Gutierrez-Roig, M. (2020). Street-Frontage-Net: urban image classification using deep convolutional neural networks. International Journal of Geographical Information Science, 34(4), 681–707. https://doi.org/10.1080/13658816.2018.1555832
31. Dastour, H., & Hassan, Q. K. (2023). A Comparison of Deep Transfer Learning Methods for Land Use and Land Cover Classification. Sustainability (Switzerland), 15(10). https://doi.org/10.3390/su15107854
32. Abijith, D., & Saravanan, S. (2022). Assessment of land use and land cover change detection and prediction using remote sensing and CA Markov in the northern coastal districts of Tamil Nadu, India. Environmental Science and Pollution Research, 29(57), 86055–86067. https://doi.org/10.1007/s11356-021-15782-6
33. Uddin, M. S., Mahalder, B., & Mahalder, D. (2023). Assessment of Land Use Land Cover Changes and Future Predictions Using CA-ANN Simulation for Gazipur City Corporation, Bangladesh. Sustainability (Switzerland), 15(16). https://doi.org/10.3390/su151612329
34. Martins, V. S., Kaleita, A. L., Gelder, B. K., da Silveira, H. L. F., & Abe, C. A. (2020). Exploring multiscale object-based convolutional neural network (multi-OCNN) for remote sensing image classification at high spatial resolution. ISPRS Journal of Photogrammetry and Remote Sensing, 168, 56–73. https://doi.org/10.1016/j.isprsjprs.2020.08.004
35. Dhanaraj, K., & Angadi, D. P. (2022). Land use land cover mapping and monitoring urban growth using remote sensing and GIS techniques in Mangaluru, India. GeoJournal, 87(2), 1133–1159. https://doi.org/10.1007/s10708-020-10302-4
36. Tariq, A., Yan, J., & Mumtaz, F. (2022). Land change modeler and CA-Markov chain analysis for land use land cover change using satellite data of Peshawar, Pakistan. Physics and Chemistry of the Earth, 128. https://doi.org/10.1016/j.pce.2022.103286
37. Xu, L., Liu, X., Tong, D., Liu, Z., Yin, L., & Zheng, W. (2022). Forecasting Urban Land Use Change Based on Cellular Automata and the PLUS Model. Land, 11(5). https://doi.org/10.3390/land11050652
38. Rahnama, M. R. (2021, January 1). Forecasting land-use changes in Mashhad Metropolitan area using Cellular Automata and Markov chain model for 2016-2030. Sustainable Cities and Society. Elsevier Ltd. https://doi.org/10.1016/j.scs.2020.102548
39. Okwuashi, O., & Ndehedehe, C. E. (2020). Deep support vector machine for hyperspectral image classification. Pattern Recognition, 103. https://doi.org/10.1016/j.patcog.2020.107298
40. Naushad, R., Kaur, T., & Ghaderpour, E. (2021). Deep transfer learning for land use and land cover classification: A comparative study. Sensors, 21(23). https://doi.org/10.3390/s21238083
41. Zhang, X., Han, L., Han, L., & Zhu, L. (2020). How well do deep learning-based methods for land cover classification and object detection perform on high resolution remote sensing imagery? Remote Sensing, 12(3). https://doi.org/10.3390/rs12030417
42. Asortse, I., Stewart, J. C., & Davis, G. A. (2024). LAND USE CLASSIFICATION OF SATELLITE IMAGES WITH CONVOLUTIONAL NEURAL NETWORKS (CNNS). Issues In Information Systems. https://doi.org/10.48009/2_iis_2024_122
43. Guo, R., Zhao, X., Zuo, G., Wang, Y., & Liang, Y. (2023). Polarimetric Synthetic Aperture Radar Image Semantic Segmentation Network with Lovász-Softmax Loss Optimization. Remote Sensing, 15(19). https://doi.org/10.3390/rs15194802